

## Research Paper

# Neonatal Heart-Enriched miR-708 Promotes Proliferation and Stress Resistance of Cardiomyocytes in Rodents

Shengqiong Deng<sup>1,2\*</sup>, Qian Zhao<sup>1\*</sup>, Lixiao Zhen<sup>1</sup>, Chuyi Zhang<sup>1</sup>, Cuicui Liu<sup>1</sup>, Guangxue Wang<sup>1</sup>, Lin Zhang<sup>1</sup>, Luer Bao<sup>1</sup>, Ying Lu<sup>1</sup>, Lingyu Meng<sup>1,3</sup>, Jinhui Lü<sup>1</sup>, Ping Yu<sup>1</sup>, Xin Lin<sup>1</sup>, Yuzhen Zhang<sup>1</sup>, Yi-Han Chen<sup>1</sup>, Huimin Fan<sup>1</sup>, William C. Cho<sup>4</sup>, Zhongmin Liu<sup>1</sup>✉ and Zuoren Yu<sup>1,3</sup>✉

1. Key Laboratory of Arrhythmias of the Ministry of Education of China, Research Center for Translational Medicine, Translational Medical Center for Stem Cell Therapy, East Hospital, Tongji University School of Medicine, 150 Jimo Road, Shanghai 200120, China;
2. Shanghai Gongli Hospital, the Second Military Medical University, Shanghai 200120, China
3. East Hospital, Dalian Medical University, Dalian, China
4. Department of Clinical Oncology, Queen Elizabeth Hospital, Hong Kong, China.

\* Equal contribution to this work

✉ Corresponding authors: Zuoren Yu, Ph.D, E-Mail: zuoren.yu@tongji.edu.cn Tel.:+86-21-61569842 Fax: +86-21-58798999 or Zhongmin Liu, M.D, E-Mail: liu.zhongmin@tongji.edu.cn Tel.:+86-21-61569842

© Ivyspring International Publisher. This is an open access article distributed under the terms of the Creative Commons Attribution (CC BY-NC) license (<https://creativecommons.org/licenses/by-nc/4.0/>). See <http://ivyspring.com/terms> for full terms and conditions.

Received: 2016.06.14; Accepted: 2017.03.23; Published: 2017.05.02

## Abstract

Adult heart has limited potential for regeneration after pathological injury due to the limited cell proliferation of cardiomyocytes and the quiescent status of progenitor cells. As such, induction of cell-cycle reentry of cardiomyocytes is one of the key strategies for regeneration of damaged heart. In this study, a subset of miRNAs including miR-708 were identified to be much more abundant in the embryonic and neonatal cardiomyocytes than that in adult rodents. Overexpression of miR-708 promoted cellular proliferation of H9C2 cells or primary cardiomyocytes from neonatal rats or mice *in vitro*. Lipid nanoparticle delivery of miR-708 promoted myocardial regeneration and heart function recovery *in vivo*. In addition, miR-708 protected cardiomyocytes against stress-induced apoptosis under hypoxia or isoproterenol treatments. miR-708 inhibited the expression of MAPK14, which has been demonstrated arresting the cell cycle in cardiomyocytes. The cell proliferation-promoting function of miR-708 was dependent at least partly on the expression of MAPK14. These findings strengthen the potential of applying miRNAs to reconstitute lost cardiomyocytes in injured hearts, and may provide a novel miRNA candidate for promoting heart regeneration.

Key words: miR-708; cardiomyocytes; heart regeneration, MAPK14.

## Introduction

The mammalian heart has very limited regenerative capacity after pathological injury due to the terminated cell proliferation of cardiomyocytes and the quiescent status of progenitor cells in adult hearts. During cardiac development in mammals, cardiomyocytes undergo the hyperplastic to hypertrophic transition before birth. Shortly after birth, the majority of cardiomyocytes withdraws from

the cell cycle and becomes so-called terminally differentiated cells, though there is still a low rate of cardiomyocyte turnover [1, 2]. Emerging evidence indicates that adult heart may still maintain the regenerative potential, especially under certain pathological conditions because of the cell cycle reentry of cardiomyocytes and the existence of a small population of cells in adult hearts called cardiac stem

cells (CSCs) or cardiac progenitor cells (CPCs).

miRNAs are a class of small non-coding RNA molecules regulating the stability or translational efficiency of targeted messenger RNAs [3]. More than 2,000 miRNA sequences have been identified or predicted from human origin tissues or cells [4]. miRNAs are mediated by RNA-induced silencing complex (RISC) that lead to base-pairing interactions between a miRNA and the binding site of its target mRNAs mostly within the 3' untranslated region (3'UTR). miRNAs regulate diverse biological processes including cell fate determination, cell cycle progression, stem cell self-renewal and differentiation [5-7].

A few miRNAs are found to be overexpressed in the heart including miR-1, miR-133, miR-208a, miR-208b, and miR-499. These miRNAs have been reported to play important roles in regulating cardiac development, cardiovascular diseases, as well as cardiac remodeling [8]. Cardiac-specific deletion of gene *Dicer* caused postnatal lethality from progressive heart failure, in which miRNA processing was interrupted and mature miRNAs were decreased in the heart [9]. In fact, miR-1 is one of the most abundant miRNAs in heart. The miR-1 family is expressed together with members of miR-133 family. The miR-1/133a bicistronic clusters (the miR-1-1/miR-133a-2 cluster and the miR-1-2/miR-133a cluster) are critical regulators of cardiac development. A specific enrichment of miR-1 was found in embryonic stem (ES) cell-derived cardiomyocytes, but not in ES cell derived smooth muscle cells and endothelial cells. Furthermore, miR-1 promotes cardiac differentiation. When miR-1 is overexpressed in human pluripotent stem cells, it will enhance the expression of key cardiac transcriptional factors and sarcomeric genes [10]. On the other hand, the miR-133 family is muscle-specific. Absence of miR-133a expression resulted in ectopic expression of smooth muscle genes in the heart and aberrant cardiomyocyte proliferation. It was reported that miR-133a-1 and miR-133a-2 double-mutant mice which survive to adulthood succumbed to dilated cardiomyopathy and heart failure [11]. These findings showed the importance of miRNAs in regulating cardiac development and cardiac diseases.

In this study, miR-708 was identified to be abundant in neonatal heart while the expression level markedly reduced in rat adult heart. Overexpression of miR-708 promoted cellular proliferation and protected cells against hypoxia-induced apoptosis in H9C2 cells and primary cardiomyocytes. Lipid

nanoparticle delivery of miR-708 promoted myocardial regeneration and heart function recovery *in vivo*.

## Results

### Identification of miR-708 as a cardiomyocytes-enriched miRNA in the heart of neonatal rat

In comparison of the non-proliferative status of cardiomyocytes in adult heart, the cardiomyocytes in neonatal heart remain active, including ongoing cell division and rapid cell growth. In order to identify the key miRNAs in maintaining the active status of cardiomyocytes, quantitative real-time PCR-based miRNA profiling analyses were performed and compared in both neonatal and adult heart tissues of rat. As shown in Figure 1A and Supplemental Figure S1, a group of miRNAs was found to be differentially expressed in the neonatal hearts compared to adult hearts. 32 miRNAs were upregulated (Table 1) and 18 miRNAs were downregulated (Table 2) in the neonatal hearts compared to adult. Notably, a subset of miRNAs in Table 1, such as miR-15b, miR-17-5p, miR-18a, miR-19a and miR-302e, has been previously reported to upregulate in heart during the neonatal period [12-14] (Figure 1B), demonstrating the consistency of our result with previous studies. In addition, our analysis showed that the miR-708 expression level is 10-15 times higher in neonatal than adult (Figure 1B).

In order to isolate and purify primary cardiomyocytes from the fresh neonatal heart tissues of rat, fibroblast cells were removed. The cells were further confirmed by immunofluorescence staining with cardiomyocytes-specific marker *cardiac troponin I* (cTnI) (Figure 1C), and quantitative RT-PCR analysis with cardiomyocytes-specific markers *cardiac muscle alpha actin 1* (ACTC1), *cardiac muscle troponin T2* (cTnT2) and fibroblast-specific markers *fibroblast growth factor receptor 1* (FGFR1), *vimentin* (Figure 1D and 1E). miRNA analyses demonstrated the high level of miR-708 in cardiomyocytes while low in fibroblasts (Figure 1F). Similar results were observed for miR-1 and miR-133 (Figure 1F).

In order to compare the expression pattern of miR-708 in cardiomyocytes during heart development, hearts from day 14.5 embryos, neonatal and adult mice were collected and analyzed. As shown in Supplemental Figure S2, miR-708 was enriched in the hearts of embryos and neonatal mice, while decreased in adults.

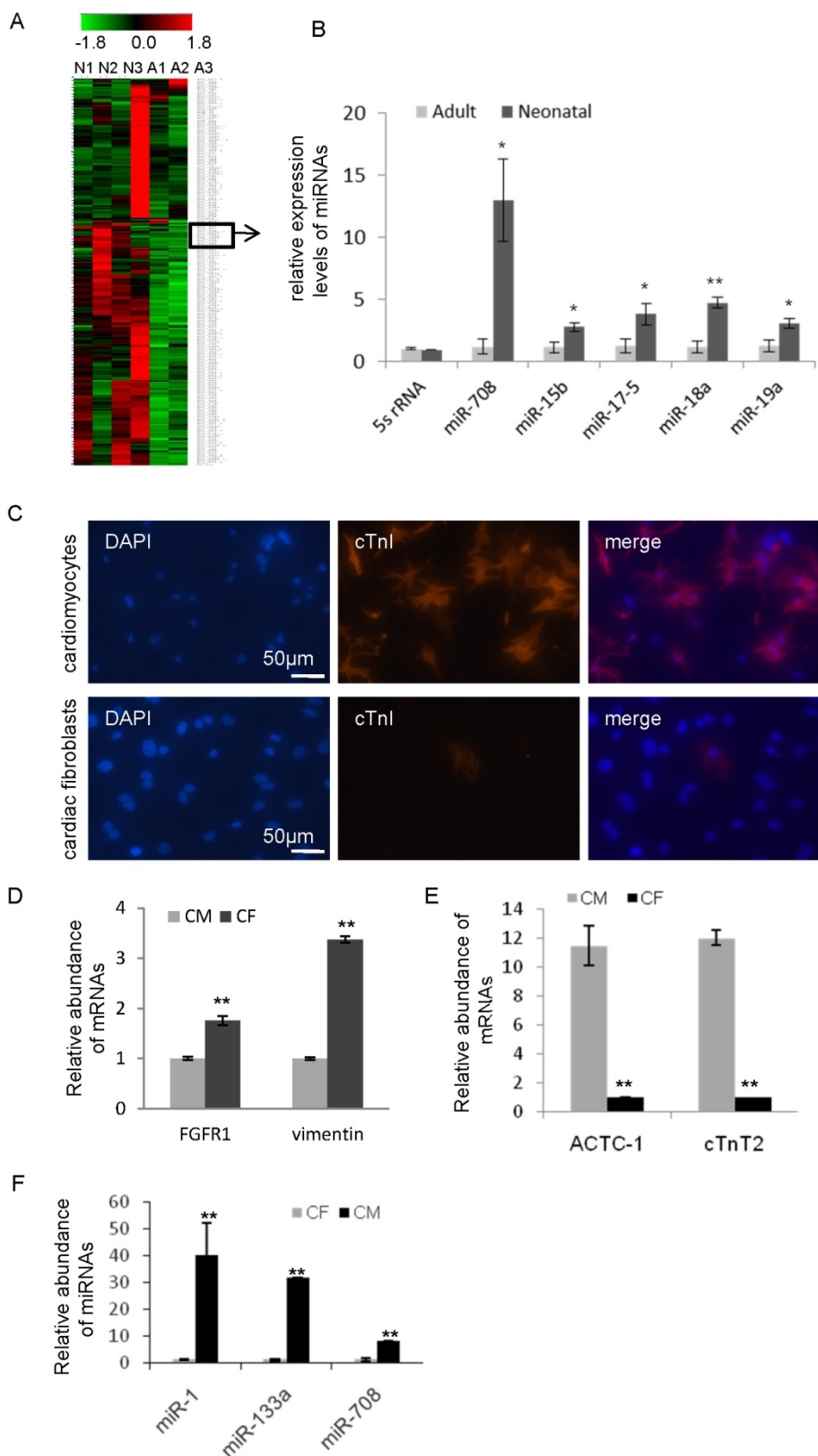


**Figure 1. miR-708 is enriched in cardiomyocytes of neonatal rats.** A: miRNA profiling analyses between three neonatal and three adult heart tissues in rats identified a subset of miRNAs including miR-708 with higher expression in the neonatal hearts compared to adults. A: adult, N: neonatal. B: The relative expression levels of indicated miRNAs in the hearts of neonatal rats and adult rats. C: Immunofluorescence staining of cardiomyocytes-specific marker cardiac troponin I (cTnI) in cardiomyocytes and fibroblast cells isolated from fresh hearts of neonatal rats. D: Quantitative analysis of fibroblast-specific markers *fibroblast growth factor receptor 1* (FGFR1) and *vimentin* in the isolated primary cardiomyocytes and fibroblast cells. E: Quantitative analysis of cardiomyocytes-specific markers *cardiac muscle alpha actin 1* (ACTC1) and *cardiac muscle troponin T2* (cTnT2) in the isolated primary cardiomyocytes and fibroblast cells. F: A miRNA quantitative analysis demonstrated the high expression of miR-1, miR-133 and miR-708 in cardiomyocytes while low in fibroblasts. CM: cardiomyocytes, CF: cardiac fibroblast cells. Data are mean ± SEM (n=3). \*p<0.05, \*\*p<0.01.

**Table 1.** Upregulated miRNAs in the hearts of neonatal rats compared to adult

miRNA ID	Fold change (adult/neo)	p value	miRNA ID	Fold change (adult/neo)	p value
miR-30c	0.454	0.049	miR-490	0.243	0.013
miR-199a	0.433	0.038	miR-191	0.239	0.014
miR-652	0.422	0.033	miR-371b-3	0.224	0.032
miR-514-5	0.406	0.029	miR-18a	0.214	0.009
miR-181b	0.405	0.053	miR-18b	0.212	0.006
miR-548a	0.396	0.012	miR-592	0.202	0.002
miR-503	0.394	0.051	miR-483	0.185	0.025
miR-15b	0.363	0.028	miR-148b	0.184	0.023
miR-107	0.355	0.024	miR-455	0.182	0.033
miR-485	0.344	0.002	miR-708	0.180	0.054
miR-106a	0.341	0.017	miR-130b	0.153	0.003
miR-19a	0.333	0.047	miR-487	0.146	0.044
miR-93	0.326	0.015	miR-323b	0.129	0.052
miR-17-5	0.275	0.036	miR-301a	0.081	0.022
miR-487b	0.271	0.029	miR-302e	0.069	0.044
miR-127-3	0.260	0.011	miR-136	0.066	0.013

**Table 2.** Downregulated miRNAs in the hearts of neonatal rats compared to adult

miRNA ID	Fold change (adult/neo)	p value	miRNA ID	Fold change (adult/neo)	p value
miR-29b	87.049	0.000	miR-105	2.842	0.044
miR-29a	39.628	0.007	miR-27a	2.774	0.015
miR-329	9.231	0.012	miR-24	2.691	0.022
miR-150	9.162	0.050	miR-222	2.662	0.037
miR-10a	4.483	0.010	miR-23a	2.545	0.025
miR-517	3.900	0.045	miR-208a	2.507	0.001
miR-497	3.757	0.012	miR-192	2.472	0.052
miR-762	3.163	0.021	miR-486	2.438	0.054
let-7b	3.006	0.004	miR-27b	2.054	0.046

### miR-708 promoted the cellular proliferation of cardiomyocytes *in vitro*

In order to determine the effect of miR-708 on cellular proliferation in heart, H9C2, a cardiomyocyte cell line derived from the embryonic rat hearts, was applied to overexpress miR-708 *in vitro*. As shown in Figure 2A, transfection of miR-708 mimics into H9C2 cells increased the level of miR-708 remarkably. A MTT assay demonstrated the increased cell proliferation in 24h and 48h after miR-708 mimic transfection (Figure 2B). In contrary, an antisense miR-708 inhibitor decreased the miR-708 levels in H9C2 cells and suppressed the cell proliferation (Figure 2C and 2D). Ki67 staining analysis indicated a higher Ki67 positive cell proportion in the miR-708 overexpressed H9C2 cells (Figure 2E and 2F). In addition to H9C2, primary cardiomyocytes isolated from the fresh heart tissues of neonatal rats were validated by staining with cardiomyocytes-specific marker  $\alpha$ -actin 1, and transfected with miR-708 mimics followed by Ki-67 staining. As shown in

Figures 2G and 2H, miR-708 promoted the proportion of  $\alpha$ -actin / Ki-67 double positive cells.

### miR-708 protected cardiomyocytes against apoptosis

In terms of the irreversible damage of myocardial tissue caused by myocardial infarction is partly due to the prolonged ischemia and lack of sufficient oxygen, the effect of miR-708 in response to hypoxia in H9C2 cells was determined. H9C2 cells were transfected with miR-708 mimics followed by culturing under the hypoxia condition of 1% oxygen for 24 hours. Annexin V analysis was applied to detect the apoptotic and dead cells. As shown in Figure 3A and 3B, overexpression of miR-708 protected H9C2 cells against apoptosis induced by hypoxia. In addition, H9C2 cells were treated with 200 $\mu$ M isoproterenol (ISO) which can induce myocardial infarction in animals, followed by analyses of cellular apoptosis and cell death. The majority of the miR-708 overexpressed H9C2 cells stayed alive after 24h treatment with ISO, while control cells underwent apoptosis and then died (Figure 3C). A quantitative analysis indicated significant decrease in the proportion of apoptotic cells induced by ISO from ~30% in control to 10-15% in miR-708 overexpressed H9C2 (Figure 3D and 3E).

### Lipid nanoparticle delivery of miR-708 promoted myocardium regeneration and heart function recovery *in vivo*

In order to determine the effects of miR-708 *in vivo* on the cardiac regeneration after injury, a nonvirus delivery system was applied to deliver miR-708 mimics or a negative control to a mice model of heart injury induced by a daily treatment with 25mg/kg ISO through intraperitoneal injections for continuous 6 days. In Figure 4A, a neutral lipid emulsion (NLE) delivery reagent, which has been reported to be able to accumulate miRNAs in the heart [14], was used to deliver miR-708 mimics to adult mice daily for 6 days via tail-vein injections. In order to confirm the delivery of miR-708 into the hearts, both instant and long-term effects after NLE-miR-708 injection were examined. As shown in Figure 4B, an immediate detection of the miR-708 levels in the heart, kidney and lung after 3-day's continuous delivery indicated the remarkable increase of miR-708 in all three tested tissues. In addition, long-term effect on the miR-708 expression in the hearts was determined at day 16 after the mice were anaesthetized. Compared to controls, miR-708 levels still kept a little bit higher in the hearts of NLE-miR-708 group (Figure 4C).

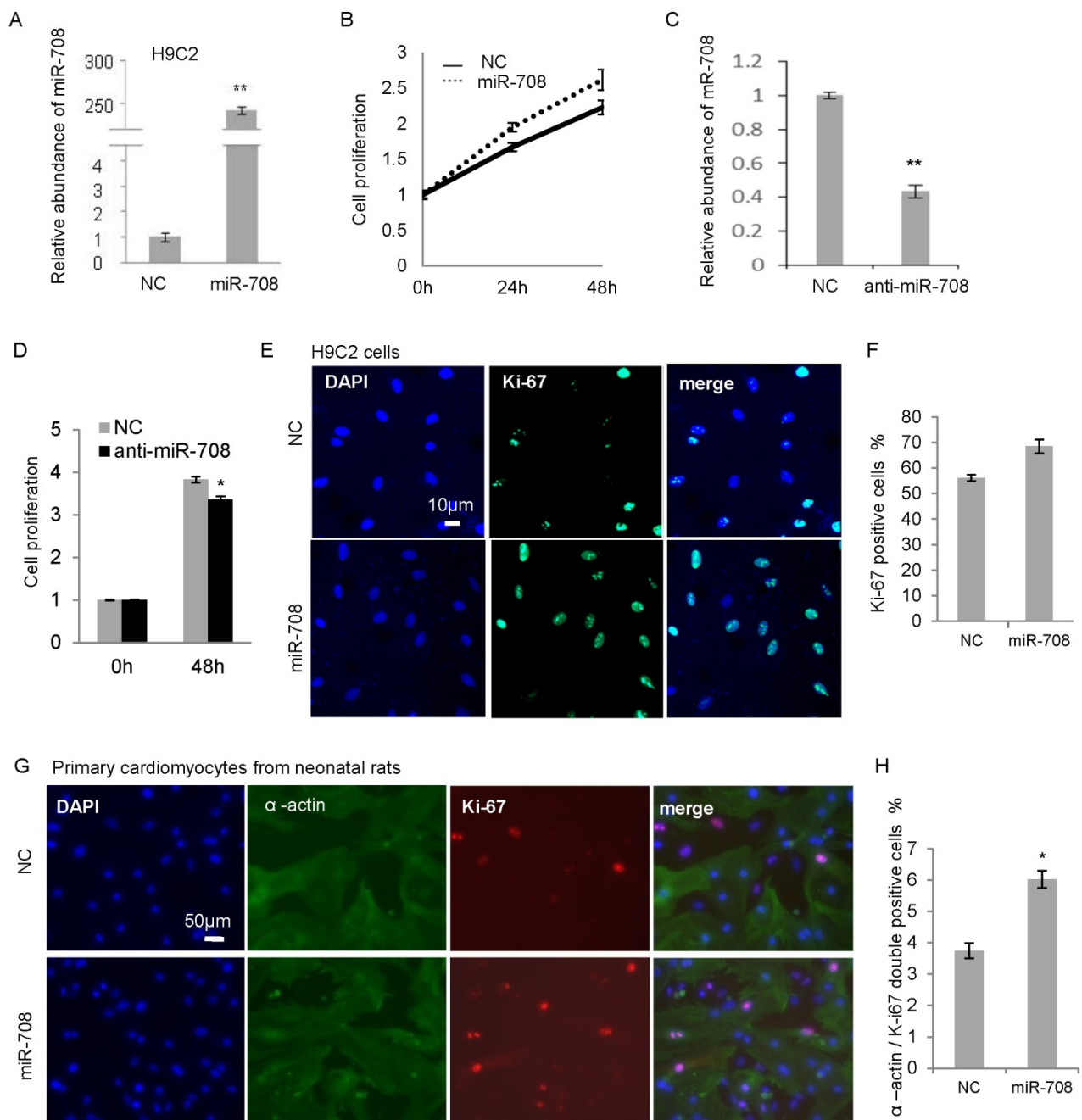


**Figure 2. miR-708 promoted the cellular proliferation of cardiomyocytes from neonatal rats.** A: Overexpression of miR-708 in H9C2 cells. B: MTT assays demonstrated the increased cell proliferation by miR-708 overexpression in H9C2 cells. C: Knockdown of miR-708 in H9C2 cells by anti-miR-708. D: Decreased cell proliferation by anti-miR-708 in H9C2 cells. E: Ki67 staining indicated a higher Ki67 positive cell proportion in miR-708 overexpressed H9C2 cells. F: Quantitative analysis of Ki67 positive cell proportion in E. G:  $\alpha$ -actin and Ki67 staining indicated a higher Ki67 positive cell proportion in the miR-708 overexpressed primary cardiomyocyte cells ( $\alpha$ -actin positive) isolated from fresh heart tissue of neonatal rats. H: Quantitative analysis of  $\alpha$ -actin / Ki67 double positive cells in G. Data are presented as mean  $\pm$  SEM (n=3). \*p<0.05, \*\*p<0.01.

The heart function of the mice was evaluated at the indicated time points through echocardiography examinations (Figure 4A, 4D) and swimming test. ISO induced heart injury in mice was confirmed by echocardiography examination (Figure 4E). After anaesthetization of the mice at day 16, the histological HE staining of the hearts was performed (Supplemental Figure S3). miRNA analysis showed that ISO-induced heart injury was associated with

increased miR-708 levels (Supplemental Figure S4), exaggerated chamber size, reduced Left ventricular contractility, decreased ejection fraction (EF%), decreased fractional shortening (FS%), increased left ventricular end diastolic volume (LVEDV) and increased left ventricular end systolic volume (LVESV), which were partly reversed by the application of miR-708 (Figure 4D-4I, Supplemental Figure S5). The EF levels decreased from ~65% in PBS

group to ~45% in ISO group, and returned to ~55% after miR-708 therapy (Figure 4F). Similar changes were observed on FS levels (Figure 4G). The increased levels of LVEDV and LVESV were seen in the heart at day 5 and day 10 after ISO treatment, which were rescued by local delivery of miR-708 (Figure 4H and 4I). A forced swim test at day 9 demonstrated the ISO-treated mice had much shorter swimming time than both PBS-treated mice and miR-708-treated ISO mice (Figure 5A and 5B), which reflected the functional recovery of the heart by local delivery of miR-708. The ratios of heart weight to body weight and heart weight to tibia length both showed

significant decrease after treatment with miR-708 (Figure 5C). Wheat Germ Agglutinin (WGA) staining to the slides from paraffin-embedded heart tissue sections stained the cell membranes and extracellular matrix of cardiomyocytes. As shown in Figure 5D and 5E, the results indicated the cardiomyocyte hypertrophy induced by ISO, which was partly rescued by miR-708 therapy. Meanwhile, Masson's Trichrome Staining demonstrated the myocardial fibrosis induced by ISO, while miR-708 application protected the cardiomyocytes against fibrosis as shown in Figure 5F and 5G.

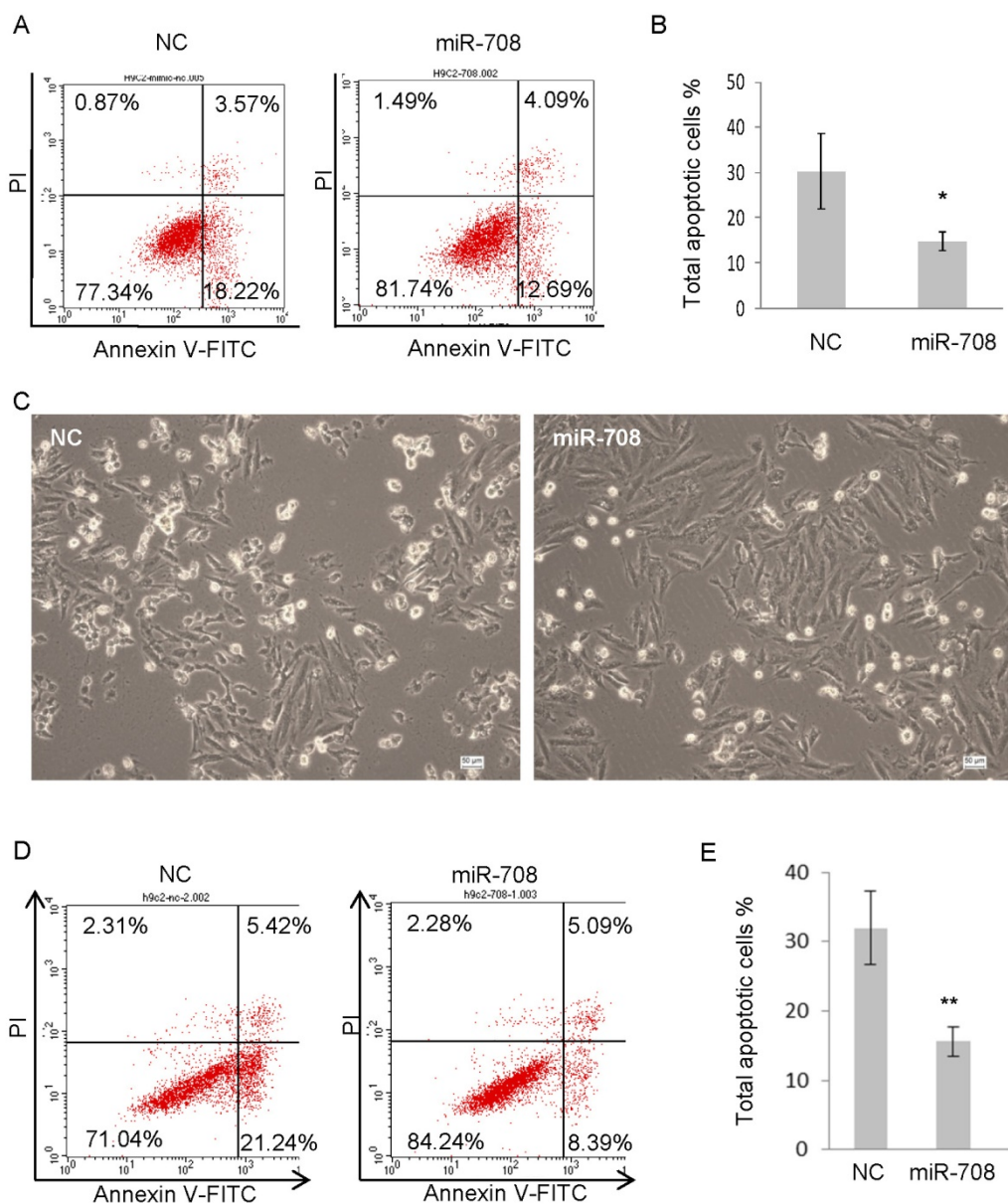


**Figure 3. miR-708 protected cardiomyocytes against apoptosis induced by hypoxia or isoproterenol.** A and B: H9c2 cells were cultured under the hypoxia condition of 1% oxygen for 24 hours with or without overexpression of miR-708, followed by Annexin V analyses (A). Bar graph showing decreased apoptotic cell percentage in the presence of miR-708 (B). C: Pictures of H9c2 cell with or without overexpression of miR-708 showing different response to 200μM isoproterenol (ISO). Scale bar 50μm. D and E: H9c2 cells were treated with 200μM ISO for 24 hours with or without overexpression of miR-708, followed by Annexin V analyses (D). Bar graph showing decreased apoptotic cell percentage in the presence of miR-708 (E). Data are presented as mean ± SEM (n=3). \*p<0.05, \*\*p<0.01.

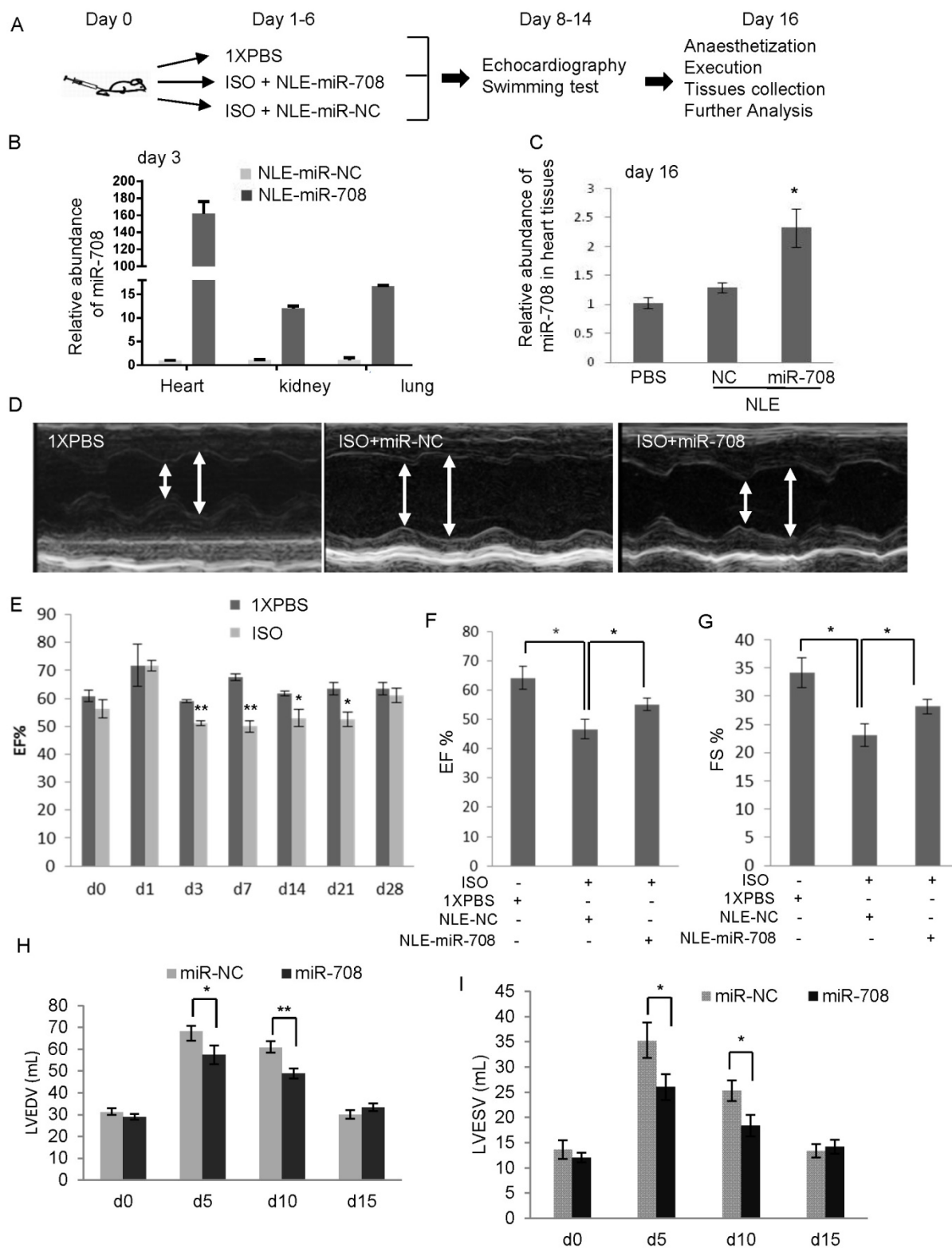


**Figure 4. miR-708 promoted cardiac regeneration in vivo.** A: Schematic representation of the procedure to deliver miR-708 mimics or a negative control using a neutral lipid emulsion (NLE) reagent into the mice with heart injury induced by ISO (n=7 for each group). The effects of miR-708 on the cardiac regeneration and recovery of heart function *in vivo* were determined. B: Detection of the instant effects of NLE-miR-708 delivery *in vivo* indicating remarkable increase of miR-708 in the heart, kidney and lung after 3-day's continuous treatment. C: The long-term effects were determined by miR-708 analysis in the hearts at day 16 after the mice were anaesthetized, indicating a little bit higher of the miR-708 levels in the hearts of NLE-miR-708 group compared to controls. D: The echocardiography examinations indicated that ISO treatments exaggerated chamber size and reduced wall thicknesses compared with PBS treated mice, which were rescued by *in vivo* delivery of miR-708. E: Time course examinations of echocardiography showing the change of EF levels in mice within four weeks after ISO treatment. PBS was used as a negative control (n=5). F: Echocardiography examinations to the mice showing the EF levels decreased from ~65% in PBS group to ~45% in ISO group, and returned to ~55% after 6-day therapy with miR-708 mimics. G: Echocardiography examinations to the mice showing the FS levels decreased from ~35% in PBS group to ~22% in ISO group, and returned to ~30% after treatment with miR-708 mimics. H,I: The increased levels of LVEDV (H) and LVESV (I) were seen in the mice at day 5 and day10 after ISO treatment, which was rescued by *in vivo* delivery of miR-708. Data are presented as mean ± SEM (n=7). \*p<0.05, \*\*p<0.01.

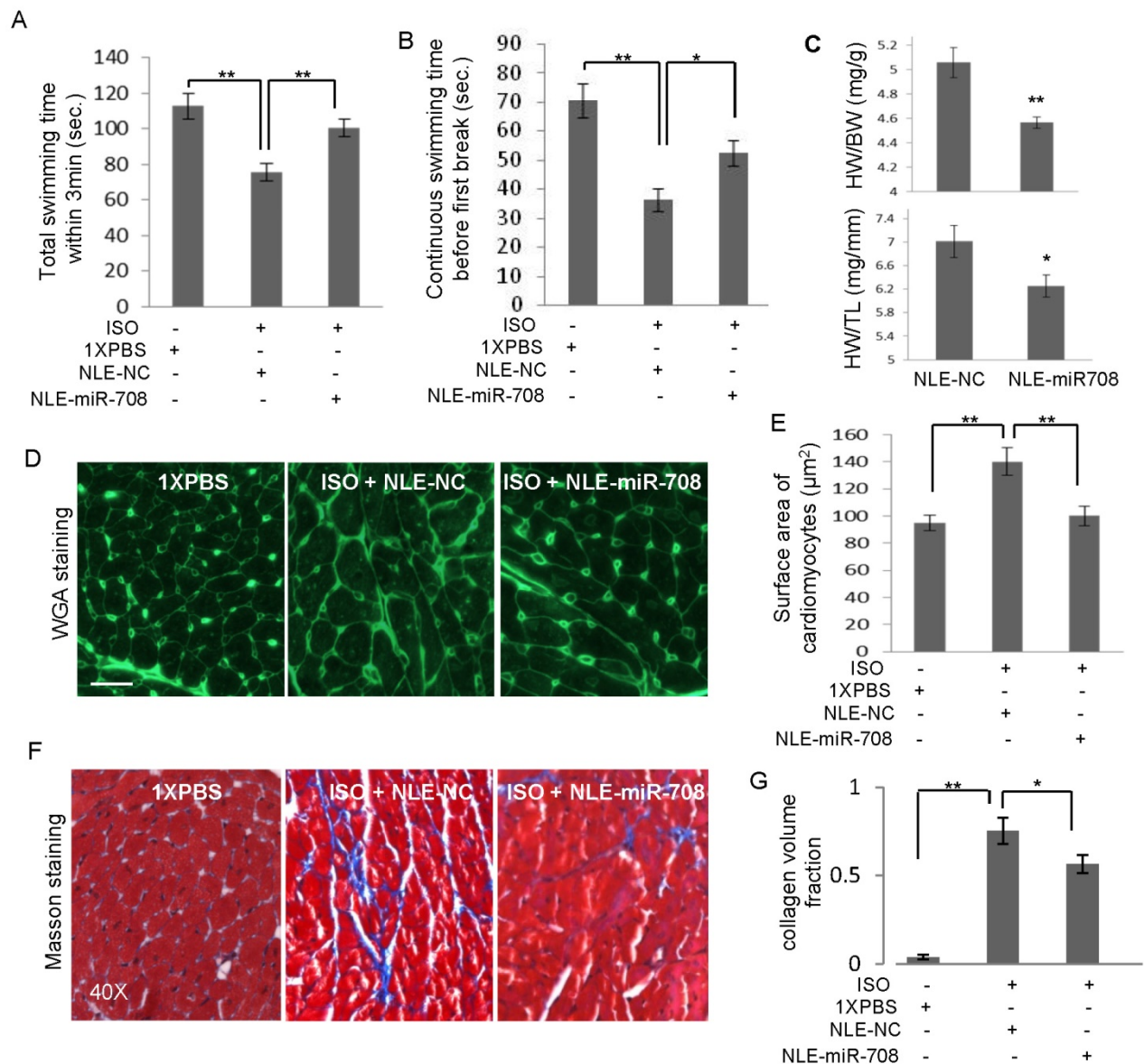


**Figure 5. miR-708 improved heart function in vivo.** A and B: A swimming test at day 9 demonstrated the ISO-treated mice had shorter swimming time within 3 min (A) and shorter swimming time before first break (B), compared to PBS control mice. miR-708 therapy improved significantly the swimming ability of the ISO-treated mice. C: miR-708 therapy decreased the ratios of heart weight to body weight and heart weight to tibia length in the ISO-treated mice. D: WGA staining showing the cardiomyocyte hypertrophy induced by ISO, which can be partly rescued by miR-708 treatment. E: Quantitative analysis of D. F: Masson's Trichrome Staining demonstrated the myocardial fibrosis induced by ISO, while miR-708 treatment protected the cardiomyocytes against fibrosis. G: Quantitative analysis of F. Data are presented as mean  $\pm$  SEM (n $\geq$ 3). \*p<0.05, \*\*p<0.01.

### miR-708 suppressed Mapk14 expression in cardiomyocytes

In order to determine the mechanism by which miR-708 regulates myocardial regeneration in rodents, a bioinformatics screening analysis using miRNA target prediction tools including TargetScan, miRanda and PITA identified 200 genes as predicted targets of miR-708 in rat by all the three tools (Figure 6A). The gene list was further narrowed down through overlapping with 66 heart failure-related genes and 54 heart defects-related genes in rat, which led to a list of four genes, Mapk14, Casp3, Mapk3 and Ppar- $\alpha$  (Figure 6A). Quantitative real-time RT-PCR

analyses demonstrated the decrease of mRNA levels of Mapk14, Casp3 and Mapk3 in cardiomyocytes after transfection with miR-708 (Figure 6B). Mapk14 mRNA was knocked down ~70% by miR-708. Notably, three binding sites to miR-708 were identified from the 3'UTR of rat Mapk14 mRNA, in which the second binding site is highly conserved with the miR-708 binding site in the mouse Mapk14 mRNA (Supplemental Figure S6). A point mutation to the conserved binding site was applied (Figure 6C). Luciferase reporter vectors carrying either wild type or point mutated MAPK14 3'UTR were assayed demonstrating the direct interaction between miR-708 and MAPK14 3'UTR (Figure 6C and 6D). The

decreased MAPK14 levels in the hearts and other tissues of mice upon the miR-708 delivery *in vivo* were confirmed at day 3 (Figure 6E) and day 16 (Figure 6F), which are consistent with the increased level of

miR-708 (Figure 4B and 4C). Western blot further demonstrated the decrease of Mapk14 protein level by miR-708 in cardiomyocytes (Figure 6G and Supplemental Figure S7).

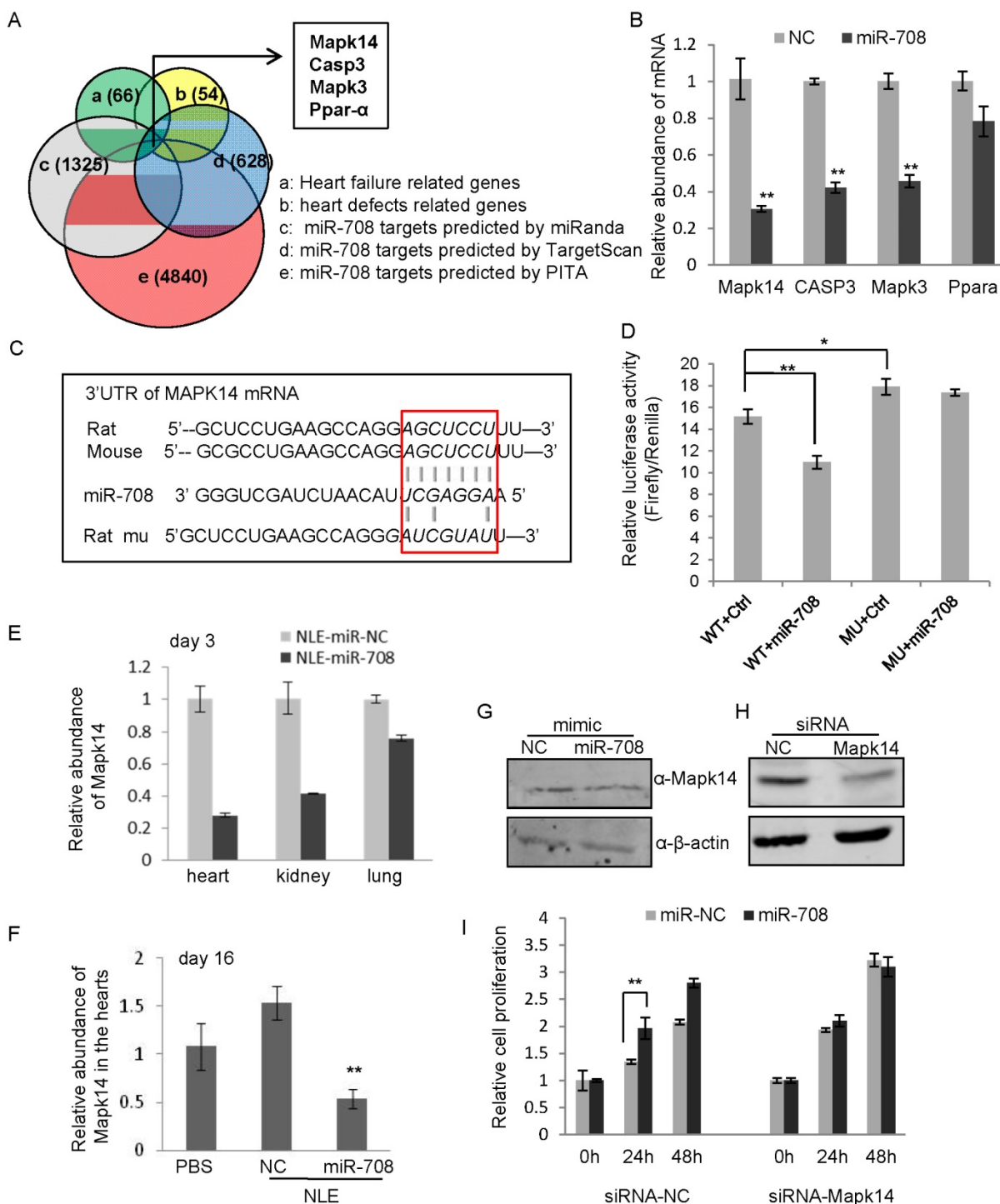


**Figure 6. miR-708 regulates Mapk14 expression in cardiomyocytes.** A: Bioinformatics screening using TargetScan, miRanda and PITA predicted miR-708 target genes, which overlapped with 66 heart failure related genes and 54 heart defects related genes, deriving Mapk14, Casp3, Mapk3 and Ppar-α as candidate target genes of miR-708 in rat cardiomyocytes. B: Quantitative real-time RT-PCR analyses demonstrated the decrease of mRNA levels of Mapk14, Casp3 and Mapk3 by miR-708 overexpression in the primary cardiomyocytes isolated from the newborn rats. C: Sequences for the WT and point mutated MAPK14 3'UTR. D: Luciferase reporter assays demonstrated the inhibition of MAPK14 3'UTR by direct interaction with miR-708. E: Decreased MAPK14 levels in the hearts, kidneys and lungs of mice upon miR-708 delivery *in vivo* after three days' miR-708 treatment. F: Decreased MAPK14 levels in the hearts of NLE-miR-708 treated mice at day 16. G: Western blot analyses demonstrating the decrease of Mapk14 protein level by miR-708 in cardiomyocytes. β-actin served as loading control. H: Western blot analyses demonstrating the knockdown of Mapk14 by siRNA in H9C2 cells. β-actin served as loading control. I: MTT analyses showed the increase of cell proliferation by miR-708 only in control H9C2 cells, but not in Mapk14 siRNA treated cells. Data are presented as mean ± SEM (n=3). \*p<0.05, \*\*p<0.01.

In order to determine whether miR-708 regulates myocardial regeneration through interaction with Mapk14, siRNA targeting rat Mapk14 was applied to H9C2 cells followed by miR-708 treatment and cell proliferation assays. As shown in Figure 6H and Supplemental Figure S8, Mapk14 expression was knocked down by siRNA. MTT analyses confirmed the increase of cell proliferation by miR-708 only in control cells, but not in Mapk14 siRNA treated cells (Figure 6I), demonstrating the induction of cardiomyocyte cell proliferation by miR-708 is dependent at least partly on the expression of Mapk14.

## Discussion

In this study, we determined the differentially expressed miRNAs in neonatal hearts compared to adult hearts of rat. We found the overexpression of a subset of miRNAs in neonatal cardiomyocytes including miR-15b, miR-17-5p, miR-18a, miR-19a, miR-302e and miR-708. In consistent with our findings, there are studies reported the upregulation of the miR-15 family, the miR-17-92 cluster and the miR-302-367 cluster in heart during the neonatal period, and demonstrated the induction of cardiomyocyte proliferation and promotion of cardiac regeneration by enforced expression of these miRNAs [12-14]. Further than these reported miRNAs, we discovered some new miRNAs with potential to promote the proliferative ability of cardiomyocytes, such as miR-708.

Through an approach of enforced overexpression, miR-708 was demonstrated to promote proliferation of cardiomyocytes *in vitro*. Moreover, miR-708 protected cardiomyocytes against apoptosis induced by either hypoxia or ISO. The results from *in vivo* assay demonstrated that local delivery of miR-708 into ISO-induced heart injury mice promoted heart regeneration and increased recovery of heart function. For the local delivery system of miRNA, a neutral lipid emulsion delivery reagent was used in this study to effectively deliver exogenous miRNA mimics into the heart via tail-vein injections. This system was successfully reported to accumulate miRNAs in the heart [14] and validated in our present study. By histological analysis and gene expression analysis, neither long-term side effects nor off-target effects of miR-708 treatment *in vivo* were observed in the current study. These findings strengthen the potential of applying miRNAs to reconstitute lost cardiomyocytes in injured hearts, and provided a novel candidate of miRNA for promoting heart regeneration.

Cardiovascular disease is a leading cause of death over the world. As we know, the proliferation

capability and turnover rate of cardiomyocytes in adult hearts are very low, the adult hearts have very limited potential for regeneration. The damaged myocardium usually undergoes degenerative remodeling process that leads to heart failure. Heart failure can be caused by many conditions which damage the heart muscle, including coronary artery disease, heart attack, cardiomyopathy, and conditions overloading work to the heart, for example, hypertension, kidney disease diabetes, etc. Although some progresses have been made in pharmacologic and device management as well as attempt of gene or cell therapy on heart failure, the mortality in heart failure patients remains significant, especially those patients over 65 years old.

Thus, the induction of cell-cycle reentry and cellular proliferation of adult cardiomyocytes may help maintaining the cardiac organ homeostasis and repair of the adult heart. Chen *et al* reported that the miR-17-92 cluster, as a critical regulator of cardiomyocyte proliferation, is required for and sufficient to induce cardiomyocyte proliferation in postnatal and adult hearts [13]. While Porrello *et al* found that the miR-15 family contributes to postnatal loss of cardiac regenerative capacity. Inhibition of the miR-15 family from an early postnatal age until adulthood increases myocyte proliferation in the adult heart and improves left ventricular systolic function after adult myocardial infarction [15]. Our study reported here on the expression of miR-708 that induced proliferation of cardiomyocytes *in vitro*, and promoted regeneration of damaged heart *in vivo*.

We found that MAPK14 is a functional target of miR-708 in cardiomyocytes. The binding site to miR-708 in the 3'UTR of mouse Mapk14 mRNA is highly conserved to one of the three miR-708 binding sites in rat Mapk14 mRNA. Luciferase reporter assay and gene expression analysis demonstrated that miR-708 suppresses MAPK14 expression, thereby reduces MAPK14 activity in cells. More specifically, we demonstrated that the function of miR-708 in regulation of cardiomyocyte proliferation was at least partly mediated by MAPK14. Whereas terminally differentiated cardiomyocytes in adult heart have diminished capacity to proliferate and regenerate. Emerging evidence indicated that MAPK14 is associated with cell cycle arrest in cardiomyocytes. Inhibition of MAPK14 activity can induce cell cycle reentry in adult myocytes. Therefore, MAPK14 inhibition by miR-708 or other molecules may represent a strategy to promote cardiac regeneration in response to injury [16-18].

In addition, MAPK14 is associated with apoptosis. Activation of MAPK14 by stress factors may lead to apoptosis by upregulating

apoptosis-related proteins. It was suggested that MAPK14 activation is pro-apoptotic in cardiomyocytes. Increased activity of MAPK14 has been observed in animal models of heart failure and myocardial biopsies from heart failure patients. MAPK14 inhibitors reduce apoptosis in cardiac cells in response to several stimuli [19-21]. Regarding to our finding that miR-708 reduced stressor-induced apoptosis in cardiomyocytes, most likely the apoptosis regulation by miR-708 may be mediated by MAPK14.

In addition to MAPK14, in airway smooth muscle (ASM) cells, other genes such as CD38 and inflammation related cytokines including CCL11, CXCL10, CCL2 and CXCL8 were suppressed in expression by miR-708 overexpression [22, 23]. In term of function, miR-708 may regulate inflammation, contractility and proliferation of ASM cells by regulating JNK MAPK and MKP-1/PI3K/AKT signaling pathways [23]. These studies may be suggestive of the involvement of MAP kinase and PI3 kinase signaling during the miR-708-regulated cell proliferation in cardiomyocytes in addition to the inhibition of MAPK14, although further experimental confirmation is required.

Besides determination of the miR-708-MAPK14 interaction, cardiomyocyte proliferation was shown by Ki-67 immunostaining with heart tissue slides from the miRNA treated mice. Unfortunately no Ki-67+ cardiomyocytes were observed in adult hearts mainly due to the very limited proliferation capacity of adult cardiomyocytes. Thus, we think it is more likely that miR-708 may reactivate the quiescent progenitor cells and promote proliferation of the freshly differentiated cardiomyocytes in adult hearts. Although this has not been demonstrated yet by experimental assays *in vivo*, our previous work has indicated the differentiation induction of cardiac progenitor cells to cardiomyocytes *in vitro* [24].

In summary, our findings not only demonstrated miR-708 playing a key role in the regulation of cardiomyocyte proliferation, cardiac repair and regeneration, but also linked the function of miR-708 and MAPK14 in cardiomyocyte proliferation and apoptosis. Furthermore, it has potential for heart regeneration therapy.

## Materials and Methods

### Animals and Treatments

Animal studies were approved by the Institutional Animal Care and Use Committee of the Tongji University for Laboratory Animal Medicine. Fisher (F344) rats were provided by Shanghai Lab. Animal Research Center [SCXK (Shanghai)]. 8- to

10-week-old C57BL/6J mice were purchased from Silaike Animal Company (Shanghai, China). Before treatment, all animals were screened for the baseline determination of echocardiography. Cardiac injury was induced by intraperitoneal injections of 25mg/kg of isoproterenol (Sigma) once daily for 6 days. Control animals received same volume of 1×PBS. Both isoproterenol and control mice were echocardiographed at day 0, 5, 10 and 15 to evaluate the heart function. At day 16, all mice were sacrificed; tissues were harvested for further analysis.

### Cells and cell culture

Cell line H9C2 was purchased from ATCC and maintained in DMEM medium with 10% of fetal bovine serum (FBS), penicillin (100U/ml) and streptomycin (100µg/ml). Cardiomyocytes from newborn rats or mice were prepared by collagenase II digestion and cultured in DMEM/M199 medium with 10% FBS, penicillin (100U/ml) and streptomycin (100µg/ml). The cardio fibroblasts and cardiomyocytes were separated using differential adhesion, and further confirmed by immunofluorescence staining with myocardial markers.

### Oligos and transfection

All siRNAs, miR-708 mimic, anti-miR-708 and negative control oligoes were synthesized by GenScript (Nanjing, China). Primer sequences for quantitative analysis of mRNAs are available upon request. The target sequence for Mapk14 siRNA: 5' GGACCTCCTTATAGACGAA 3'. The target sequence for negative control siRNA: 5' AGTCGCATACCTCGACAATAAT 3'. The miRNA mimic sequences for WT and mutation miR-708 are: WT, 5' AAGGAGCUUACAAUCUAGCUGGG 3'; mutation, 5' AUCGACCUUACUAUCUAGCUGGG 3'. The HiPerFect transfection reagent from Qiagen was used for cell transfection following the manufacturer's instructions. Final concentration of 30 nM of small RNA oligoes was used for all *in vitro* assays.

### miRNA QRT-PCR analysis

An M&G miRNA Reverse Transcription Kit (miRGenes, Shanghai, China) was used to prepare the first strand cDNA of miRNAs following the manufacturer's instruction. 100ng of purified total RNA from each sample was used for miRNA measurement. After reverse transcription, the cDNA was diluted 1:1,000 for real-time PCR. Forward primer sequences for real-time PCR of miRNAs were: miR-1: 5' cctggaatgtaaagaagtatg 3'; miR-708: 5' gagcuuacaaucucagcug 3'; miR-15b: 5' tagcagcacatcatggtt 3'; miR-17-5p: 5' caaagtgcctacagtgc

3'; miR-18a: 5' ggtgcatctagtgcagatag 3'; miR-19a: 5' cctgtgcaaatctatgcaa 3'; miR-133a: 5' ttggtcccctcaacc 3' and 5s rRNA: 5' agtacttgatgggagaccg 3'. A universal reverse primer was provided by miRGenes. The SYBR Green Master Mix was purchased from ABI (Applied Biosystem, Life Technologies). The ABI 7900 HT Sequence Detection System (Applied Biosystem, Life Technologies) was used for quantitative real time PCR assay. 5s rRNA was used for normalization.

### miRNA profiling analysis in neonatal and adult rat hearts

Total RNA was isolated from hearts with Trizol reagent (Life Technologies). The cDNA was prepared as described above. The miRNA profiling analyses were performed with the quantitative real-time PCR based miRNA panel which contains 365 miRNAs and 5 reference small RNAs (miRGenes, Shanghai, China). The data was analyzed by Mev (version 4.9) software.  $p < 0.05$  was considered as significant.

### Western blot analysis

Cell lysates (50 $\mu$ g) were separated by 10% SDS-PAGE. The proteins were transferred to nitrocellulose membrane. After blocking in 5% milk (w/v) at room temperature for one hour, the membranes were incubated at 4°C overnight with primary antibodies (1:2,000). Following PBST washing for three times with 10 min for each, the membranes were incubated with secondary antibodies (1:3,000) at room temperature for 1 hour followed by washing and staining. The antibodies below were used: anti-Mapk14 (#9212, Cell Signaling) and anti- $\beta$ -actin (sc-47778, Santa Cruz Biotechnology).

### Cell proliferation assay

4x10<sup>3</sup> cells/well were seeded into 96-well plate. At the indicated time points, 3-(4, 5-dimethylthiazol-2-yl)-2, 5-diphenyltetrazolium (MTT) was used to stain cells for measuring cell proliferation.

### Assessment of myocyte cross-sectional area

Slides from paraffin-embedded heart tissue were incubated with Alexa Fluor 488 conjugated wheat germ agglutinin (W11261, Fisher Scientific) for 45 minutes at room temperature. The mean cross-sectional area was calculated from ~150 cardiomyocytes in 5 randomly selected fields from 3 individual sections per group by using Image J software (National Institutes of Health, USA).

### Masson staining

Slides from paraffin-embedded heart tissues were stained for fibrosis analysis with Masson's trichrome following standard method. The ratio of interstitial fibrosis to the total left ventricular area was

calculated based on 20 randomly selected microscopic fields in three individual sections per group. Images were captured by a fluorescence microscopy (Leica, Germany), and analyzed with Image J software.

### Immunofluorescence

Adherent cells were fixed with 4% paraformaldehyde for 15 min, permeabilized with 0.1% Triton X-100 and then blocked with 1% BSA for 1h. After incubation with primary antibody (1:10 to 1:100 dilution) overnight at 4°C, FITC-conjugated goat anti rabbit IgG (ab6717, Abcam, 1:200 dilution) was used as secondary antibody. 6-diamidino-2-phenylindole (DAPI) was used for nuclear counterstaining. The slides were photographed using fluorescence microscopy (Leica, Germany). Primary antibodies: anti-cTnI (ab47003, Abcam), anti-Ki67 (ab15580, Abcam), anti- $\alpha$ -actin (A7811, Sigma).

### Cellular apoptosis assay

Cells were treated by either Hypoxia condition (1% O<sub>2</sub>, 94% N<sub>2</sub>, 5% CO<sub>2</sub>) for 24 hours or ISO (200 $\mu$ M) for 24 hours, followed by Annexin V staining and FACS analysis according to the manufacturer's instructions.

### Systemic delivery of miRNA mimics using a neutral lipid emulsion

RNA-LANCER II lipid miR708 mimics and control were packaged as using MaxSuppressor in vivo RNA-LANCER II (3410-01, Bioo Scientific) according to the manufacturer's instructions and delivered to adult mice (8 weeks old) with a daily dose of 0.4 mg/kg body weight NLE-formulated miRNA mimics via tail vein injection. To identify the effect of miRNA mimics on myocardial injury induced by ISO, miR-708 mimics or miRNA mimic control was administered daily for 6 days with ISO treatment.

### Luciferase reporter assay

H9C2 cells were seeded on 12-well plates at a density of 1x10<sup>5</sup> cells/well. Then cells were transfected using lipofectamine 2000 (Invitrogen) with 1.0  $\mu$ g WT or mutated pMIR-Reporter Luciferase MAPK14 3'UTR and 0.2 $\mu$ g of Renilla plasmid on the second day. 24 hours after transfection, luciferase activities were measured using Dual-Luciferase Reporter Assay System (Promega) by AutoLumat.

### Statistical analysis

Data are presented as mean  $\pm$  SEM. The standard two-tailed student's *t*-test was used for analysis, in which  $p < 0.05$  was considered statistical significant.

## Supplementary Material

Supplementary figures and tables.

<http://www.thno.org/v07p1953s1.pdf>

## Acknowledgements

This work was supported by grant 13JC1401702 and 124119a7100 from Science and Technology Commission of Shanghai Municipality, grant 2016YFA0101202 from the National Key Research and Development Program of China Stem Cell and Translational Research, Science Foundation PWRq2016-35 for The Excellent Youth Scholars of Pudong Health Bureau of Shanghai, Health Industry Project PW2013E-1 from Pudong Health Bureau of Shanghai, and grants 81370175 and 81572593 from Natural Science Foundation of China.

## Competing Interests

The authors have declared that no competing interest exists.

## References

- Beltrami AP, Barlucchi L, Torella D, *et al.* Adult cardiac stem cells are multipotent and support myocardial regeneration. *Cell*. 2003; 114(6):763-776.
- Li F, Wang X, Capasso JM, Gerdes AM. Rapid transition of cardiac myocytes from hyperplasia to hypertrophy during postnatal development. *J Mol Cell Cardiol*. 1996; 28(8):1737-1746.
- Bartel DP. MicroRNAs: genomics, biogenesis, mechanism, and function. *Cell*. 2004; 116(2):281-297.
- Li Y, Liang C, Ma H, *et al.* miR-221/222 promotes S-phase entry and cellular migration in control of basal-like breast cancer. *Molecules*. 2014; 19(6):7122-7137.
- Cui Q, Yu Z, Purisima EO, Wang E. Principles of microRNA regulation of a human cellular signaling network. *Mol Syst Biol*. 2006; 2:46.
- Tili E, Michaille JJ, Gandhi V, Plunkett W, Sampath D, Calin GA. miRNAs and their potential for use against cancer and other diseases. *Future Oncol*. 2007; 3(5):521-537.
- Calin GA, Croce CM. MicroRNA signatures in human cancers. *Nat Rev Cancer*. 2006; 6(11):857-866.
- Small EM, Olson EN. Pervasive roles of microRNAs in cardiovascular biology. *Nature*. 2011; 469(7330):336-342.
- Chen JF, Murchison EP, Tang R, *et al.* Targeted deletion of Dicer in the heart leads to dilated cardiomyopathy and heart failure. *Proc Natl Acad Sci U S A*. 2008; 105(6):2111-2116.
- Lu TY, Lin B, Li Y, Arora A, *et al.* Overexpression of microRNA-1 promotes cardiomyocyte commitment from human cardiovascular progenitors via suppressing WNT and FGF signaling pathways. *J Mol Cell Cardiol*. 2013; 63:146-154.
- Liu N, Bezprozvannaya S, Williams AH, Qi X, Richardson JA, Bassel-Duby R, Olson EN. microRNA-133a regulates cardiomyocyte proliferation and suppresses smooth muscle gene expression in the heart. *Gene Dev*. 2008; 22(23):3242-3254.
- Porrello ER, Johnson BA, Aurora AB, *et al.* MiR-15 family regulates postnatal mitotic arrest of cardiomyocytes. *Circ Res*. 2011; 109(6):670-679.
- Chen J, Huang ZP, Seok HY, *et al.* mir-17-92 cluster is required for and sufficient to induce cardiomyocyte proliferation in postnatal and adult hearts. *Circ Res*. 2013; 112(12):1557-1566.
- Tian Y, Liu Y, Wang T, *et al.* A microRNA-Hippo pathway that promotes cardiomyocyte proliferation and cardiac regeneration in mice. *Sci Transl Med*. 2015; 7(279):279ra238.
- Porrello ER, Mahmoud AI, Simpson E, *et al.* Regulation of neonatal and adult mammalian heart regeneration by the miR-15 family. *Proc Natl Acad Sci U S A*. 2012; 110(1):187-192.
- Yokota T, Wang Y. p38 MAP kinases in the heart. *Gene*. 2015; 575(2 Pt 2):369-376.
- Engel FB, Schebesta M, Duong MT, Lu G, Ren S, Madwed JB, Jiang H, Wang Y, Keating MT. p38 MAP kinase inhibition enables proliferation of adult mammalian cardiomyocytes. *Gene Dev*. 2005; 19(10):1175-1187.
- Engel FB. Cardiomyocyte proliferation: a platform for mammalian cardiac repair. *Cell Cycle*. 2005; 4(10):1360-1363.
- Mackay K, Mochly-Rosen D. An inhibitor of p38 mitogen-activated protein kinase protects neonatal cardiac myocytes from ischemia. *J Biol Chem*. 1999; 274(10):6272-6279.
- Sharov VG, Todor A, Suzuki G, Morita H, Tanhecho EJ, Sabbah HN. Hypoxia, angiotensin-II, and norepinephrine mediated apoptosis is stimulus specific in canine failed cardiomyocytes: a role for p38 MAPK, Fas-L and cyclin D1. *Eur J Heart Fail*. 2003; 5(2):121-129.
- Kyoi S, Otani H, Matsuhisa S, *et al.* Opposing effect of p38 MAP kinase and JNK inhibitors on the development of heart failure in the cardiomyopathic hamster. *Cardiovasc Res*. 2006; 69(4):888-898.
- Dileepan M, Sarver AE, Rao SP, Panettieri RA, Jr., Subramanian S, Kannan MS. MicroRNA Mediated Chemokine Responses in Human Airway Smooth Muscle Cells. *PLoS one*. 2016; 11(3):e0150842.
- Dileepan M, Jude JA, Rao SP, Walseth TF, Panettieri RA, Subramanian S, Kannan MS. MicroRNA-708 regulates CD38 expression through signaling pathways JNK MAP kinase and PI3K/AKT in human airway smooth muscle cells. *Respirology*. 2014; 15:107.
- Deng S, Zhao Q, Zhou X, Zhang L, Bao L, Zhen L, Zhang Y, Fan H, Liu Z, Yu Z. Neonatal heart-enriched miR-708 promotes differentiation of cardiac progenitor cells in rat. *Int J Mol Sci*. 2016; 17(6):E875.